Hard exclusive photoproduction of Φ mesons

C. F. Berger*
Department of Physics and Astronomy, SUNY at Stony Brook, Stony Brook, New York 11794-3800

W. Schweiger†
Institut für Theoretische Physik, Universität Graz, Universitätsplatz 5, A-8010 Graz, Austria
(Received 27 October 1999; published 10 May 2000)

We calculate the differential cross section and single-polarization observables for the reaction $\gamma p \to \Phi p$ within perturbative QCD, treating the proton as a quark-diquark system. The phenomenological couplings of gauge bosons to (spatially extended) diquarks and the quark-diquark distribution amplitude of the proton are adopted from previous investigations of baryon form factors and two-photon processes. Going beyond leading order, we take into account hadron-mass effects by means of a systematic expansion in the small parameter (hadron mass/ photon energy). With the Φ-meson distribution amplitude taken from the literature our predictions for the differential cross section at $|t| \gtrsim 4$ GeV^2 seem to provide a reasonable extrapolation of the low-t data and are also comparable in magnitude with the results of a two-gluon exchange model in which the gluons are considered as a remnant of the Pomeron. For momentum transfers of a few GeV hadron-mass effects appear still to be sizeable.

PACS number(s): 13.60.Le, 12.38.Bx

I. INTRODUCTION

In the course of the last few years exclusive photo- and electroproduction of neutral vector mesons (ρ, ω, Φ, J/Ψ) at intermediate and high energies has attained increased theoretical interest, which has been stimulated by corresponding experimental efforts at the Continuous Electron Beam Accelerator Facility (CEBAF) [1] and the DESY ep collider HERA [2]. The aim of the HERA experiments is a more fundamental understanding of Pomeron phenomenology in terms of QCD. Vector-meson dominance in combination with Pomeron exchange proves to be very successful in describing diffractive photo- and electroproduction of neutral vector mesons, provided the energy is the only large scale in the process [3]. In their approach Donnachie and Landshoff [4] assume that the Pomeron couples directly to on-shell quarks in the vector meson and the proton, respectively. A QCD-inspired version of Pomeron exchange, in which the Pomeron is replaced by two non-perturbative (Abelian) gluons, goes back to the same authors [5] and is usually termed a ''soft Pomeron.'' In the limit $t \to 0$ the soft-Pomeron exchange becomes very similar to the usual Pomeron exchange. This can be used to interpret the form factor at the quark-Pomeron vertex [5]. However, if, in addition to the energy another scale, such as the photon virtuality or the mass of the vector meson, becomes large, perturbative QCD effects tend to enter the game. For large photon virtuality (and small values of Mandelstam t) perturbative QCD becomes applicable due to a factorization theorem which has been proved in Ref. [6]. The three building blocks of the factorization formula are the hard photon-parton scattering amplitude, the distribution amplitude of the vector meson and finally a skewed gluon distribution of the proton. As a link between hard inclusive and exclusive reactions which generalizes the ordinary parton distributions, skewed parton distributions have recently attracted a great amount of interest (see, e.g., Ref. [7] and references therein). Electroproduction with highly virtual photons thus offers a possibility to study such skewed parton distributions. Within this perturbative formalism for vector-meson electroproduction with highly virtual photons the two-gluon aspect of the Pomeron emerges automatically in a form which is related to the skewed gluon distribution in the proton.

One of the aims of photoproduction experiments at CEBAF is, on the other hand, to understand the transition from non-perturbative to perturbative production mechanisms. In the case of photoproduction the transverse momentum transfer $p_\perp^2 \approx tu/s$ has to be large in order for perturbative QCD to become applicable. The pertinent factorization formula, which in general holds for arbitrary exclusive hadronic processes at large transverse momenta, is the result of a leading-order perturbative analysis. It represents a hadronic amplitude as a convolution integral of a hard-scattering amplitude with distribution amplitudes (DAs) [8]. The process-dependent hard-scattering amplitude is perturbatively calculable and represents the scattering of hadronic constituents in collinear approximation. The process-independent DAs contain the non-perturbative bound-state dynamics of the hadronic constituents. There is no doubt that this hard-scattering approach (HSA) gives the correct description of exclusive hadronic processes in the limit of asymptotically large momentum transfer. But there is increasing evidence that the pure perturbative contribution is not the dominant one at experimentally accessible momentum transfers. A reasonable reproduction of the existing exclusive large-t data is only achieved with very end-point-concentrated hadron DAs, such as those proposed by Chernyak and Zhitnitsky on the basis of QCD sum rules [9]. Such DAs, however, turn out to be problematic for a perturbative calculation since they enhance contributions from the soft end-point regions in the convolution integral [10]. Some improvement with regard to the consistency of the perturbative calculation can be achieved by applying a modified factorization scheme in which

*Email address: carola.berger@sunysb.edu
†Email address: wolfgang.schweiger@kfunigraz.ac.at

transverse-momentum effects and Sudakov suppressions are included. But this leads to a substantial reduction of the perturbative contribution [11]. For the pion an end-point concentrated DA meanwhile seems even to be ruled out by the recent CLEO data [12] for the $\pi\gamma$-transition form factor, since it provides a much too large perturbative result. On the other hand, it has been shown recently for electromagnetic nucleon form factors [13] and for wide-angle Compton scattering [7,14] off protons that the existing data can be saturated by soft overlap contributions. Furthermore, these contributions can be modeled by a nucleon light-cone wave function which gives rise to a distribution amplitude close to the asymptotic one. This, however, implies that the perturbative contribution becomes small.

The approach which we are going to apply for hard exclusive photoproduction of Φ mesons is still based on the HSA but includes also a certain amount of soft physics which is modeled by means of diquarks. Diquarks may be considered as an effective way to account for quark-quark correlations in baryon wave functions. Part of the soft overlap contributions are then absorbed into phenomenologically parametrized diquark form factors which occur at the gauge-boson diquark vertices. This HSA-based diquark model has already been applied successfully to other photon-induced hadronic reactions like magnetic and electric baryon form factors in the space-like [15] and time-like region [16], real and virtual Compton scattering [17,18], two-photon annihilation into baryon-antibaryon [16,18], and photoproduction of K mesons [19]. Further applications of the diquark model include the charmonium decay $\eta_c \to p\bar{p}$ [16] and the calculation of Landshoff contributions in elastic proton-proton scattering [20]. The purpose of the present investigation is to extend this foregoing work to $\gamma p \to \Phi p$. The reason why we concentrate on the Φ channel is that it is cleaner and simpler than photoproduction of ρ or ω mesons. Within the HSA the valence Fock state of the Φ, i.e. the s-$\bar{s}$ state, can only be produced via the exchange of two gluons between the Φ and the proton. Quark exchange could only happen via the knockout of an s-$\bar{s}$ pair from the strange-quark sea in the nucleon which is, however, power suppressed within the HSA.

In the following section we start with a short outline of the diquark model, show how Feynman diagrams are properly grouped according to their propagator singularities (Sec. II B), sketch how we deal with the propagator singularities numerically (Sec. II C), and present our treatment of hadron-mass effects (Sec. II D). Section III summarizes how photoproduction of vector mesons is described in terms of helicity amplitudes. Furthermore, the fixed-angle scaling behavior of these helicity amplitudes is discussed and related to the treatment of mass effects. Analytical expressions for the hard part of the hadron-helicity-conserving amplitudes are also given in this section. Our predictions for photoproduction observables along with predictions from Pomeron and soft-Pomeron exchange are presented in Sec. IV. At the end of this section we comment on the prospects of extending our calculation to photoproduction of J/Ψ mesons. Finally, a summary and concluding remarks can be found in Sec. V.

II. FORMALISM

A. Hard-scattering formalism with diquarks

As already mentioned before, within the HSA an exclusive scattering amplitude at large momentum transfer is expressed as a convolution integral of a hard-scattering amplitude with hadron distribution amplitudes [8]. For the photoproduction reaction $\gamma p \to \Phi p$, which we are interested in, this integral takes the particular form

$$M_{\{\lambda\}}(\hat{s},\hat{t}) = \int_0^1 dx_1 dy_1 dz_1 \phi^{\Phi\dagger}(z_1,\tilde{p}_\perp)\phi^{p\dagger}(y_1,\tilde{p}_\perp)\hat{T}_{\{\lambda\}}(x_1,y_1,z_1;\hat{s},\hat{t})\phi^{p}(x_1,\tilde{p}_\perp). \tag{2.1}$$

The distribution amplitudes ϕ^H are probability amplitudes for finding the valence Fock state in the hadron H with the constituents carrying certain fractions of the momentum of their parent hadron and being collinear up to a factorization scale $\tilde{p}_\perp$. In our model the valence Fock state of an ordinary baryon is assumed to consist of a quark (q) and a diquark (D). We fix our notation in such a way that the momentum fraction appearing in the argument of ϕ^H is carried by the quark—with the momentum fraction of the other constituent (either diquark or antiquark) it sums up to 1 (cf. Fig. 1). For our actual calculations the (logarithmic) $\tilde{p}_\perp$ dependence of the DAs is neglected throughout since it is of minor importance in the restricted energy and momentum-transfer range we are interested in. The hard scattering amplitude $\hat{T}_{\{\lambda\}}$ is calculated perturbatively. Intrinsic transverse momenta of the constituents are thereby neglected; i.e., one assumes that the momenta of the constituents are collinear to those of their parent hadron. $\hat{T}_{\{\lambda\}}$ consists in our particular case of all possible tree diagrams contributing to the elementary scattering process $\gamma q D \to Q\bar{Q} q D$. Eight of the, altogether, 16 diagrams which contribute to photoproduction of (heavy) quarkonia are depicted in Fig. 2. The subscript $\{\lambda\}$ of $\hat{T}$ represents a set of possible photon, proton and vector-meson helicities. For our purposes it appears to be more convenient to express the analytical results in terms of massless Mandelstam variables $\hat{s}$, $\hat{t}$, and $\hat{u}$ than in terms of the usual (massive) ones. A detailed account of our treatment of hadron-mass effects is given in Sec. II D below.

The diquark model, as applied in Refs. [15–19], comprises scalar (S) as well as axial-vector (V) diquarks. The dynamics of S and V diquarks is determined by their cou-

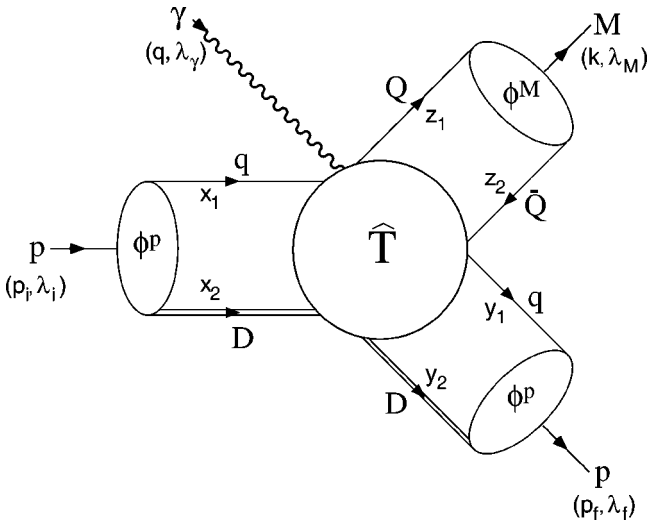

FIG. 1. Graphical representation of the hard-scattering formula, Eq. (2.1), for $\gamma p \to M p$. Here x_i, y_i, and z_i denote longitudinal momentum fractions of the constituents.

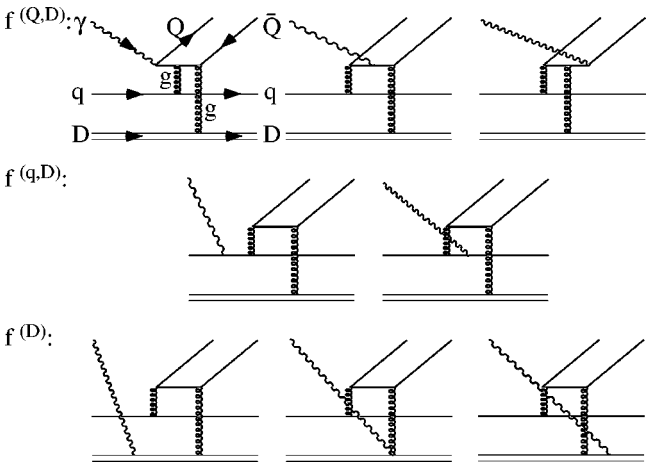

FIG. 2. Eight of the, altogether, 16 tree-level diagrams which contribute to the elementary process $\gamma q D \to Q \bar{Q} q D$. The remaining diagrams are obtained by interchanging the two gluons. We have also indicated how the diagrams are grouped to gauge invariant expressions.

pling to photons and gluons. The expressions for the photon-diquark and gluon-diquark vertices correspond (almost) to the most general form for the (parity and time-reversal invariant) coupling of a spin-1 gauge boson to a spin-0 or a spin-1 particle, respectively [15]. Thereby V diquarks are allowed to possess an anomalous (chromo)magnetic moment κ_V. In applications of the model Feynman graphs are calculated first with the corresponding Feynman rules for point-like diquarks. As a second step, Feynman graphs with $(n-2)$ gauge bosons coupling to the diquark are combined in a group which we call ''n-point contribution.'' Finally the composite nature of diquarks is taken into account by multiplying each n-point contribution with phenomenological vertex functions, the diquark form factors. The particular choice

$$F_S^{(3)}(Q^2) = \delta_S \frac{Q_S^2}{(Q_S^2+Q^2)}, \tag{2.2}$$

$$F_V^{(3)}(Q^2) = \delta_V \left(\frac{Q_V^2}{Q_V^2+Q^2} \right)^2, \tag{2.3}$$

for 3-point contributions, and

$$F_S^{(n)} = a_S F_S^{(3)}(Q^2), \tag{2.4}$$

$$F_V^{(n)} = a_V F_V^{(3)}(Q^2) \left(\frac{Q_V^2}{Q_V^2+Q^2} \right)^{(n-3)}, \tag{2.5}$$

for n-point contributions ($n \geqslant 4$), ensures that in the limit $Q^2 \to \infty$ the scaling behavior of the diquark model goes over in that of the pure quark HSA. The factor $\delta_{S(V)} = \alpha_s(Q^2)/\alpha_s(Q_{S(V)}^2)$ ($\delta_{S(V)}=1$ for $Q^2 \leqslant Q_{S(V)}^2$) provides the correct powers of $\alpha_s(Q^2)$ for asymptotically large Q^2. For the running coupling α_s the one-loop result $\alpha_s = 12\pi/25\ln(Q^2/\Lambda_{QCD}^2)$ is used with $\Lambda_{QCD}=200$ MeV. In addition α_s is restricted to be smaller than 0.5. Here a_S and a_V are strength parameters which allow for the possibility of diquark excitation and breakup in intermediate states where diquarks can be far off shell.

Having sketched how diquarks are treated perturbatively, a few words about the choice of the DAs (which incorporate the bound-state dynamics of the hadronic constituents) and the spin-flavor wave functions of the proton and the Φ are in order. If one assumes zero relative orbital angular momentum between quark and diquark and takes advantage of the collinear configuration [$p_q = x_1 p_B$ and $p_D = x_2 p_B = (1-x_1)p_B$], the valence Fock-state wave function of an octet baryon B may be written as

$$\Psi^B(p_B;\lambda) = f_S^B \phi_S^B(x_1)\, \chi_S^B\, u(p_B,\lambda) + f_V^B\, \phi_V^B(x_1)\, \chi_V^B \frac{1}{\sqrt{3}} \left(\gamma^\alpha + \frac{p_B^\alpha}{m_B} \right) \gamma_5 u(p_B,\lambda). \tag{2.6}$$

The two terms in Eq. (2.6) represent states consisting of a quark and either a scalar or a vector diquark. The pleasant feature of the covariant wave-function representation, Eq. (2.6), is that it contains, besides x_1 and α (the Lorentz index of the vector-diquark polarization vector), only baryonic quantities (momentum p_B, helicity λ, baryon mass m_B). Assuming an SU(6)-like spin-flavor dependence, the flavor functions χ_D^p for a proton take on the form

$$\chi_S^p = uS_{[u,d]}, \quad \chi_V^p = [uV_{\{u,d\}} - \sqrt{2}dV_{\{u,u\}}]/\sqrt{3}. \quad (2.7)$$

In Eq. (2.6) the color part of the quark-diquark wave function has been neglected. Since the quark-diquark state has to be a color singlet, the diquark has to be in a color antitriplet state (like an antiquark) Thus the quark-diquark color wave function is simply $\psi_{qD}^{\text{color}} = (1/\sqrt{3})\Sigma_{a=1}^{3}\delta_{aa}^{-}$.

Like the baryon wave function, Eq. (2.6), also the Q-$\bar{Q}$ wave function of a vector meson M can be represented in a covariant way:

$$\Psi^M(p_M;\lambda) = -f^M \phi^M(z_1,\lambda)\chi^M \frac{1}{\sqrt{2}}(\not{p}_M + m_M)\not{\epsilon}(\lambda), \quad (2.8)$$

with $\epsilon(\lambda)$ denoting the polarization vector of the vector meson. The flavor function of the Φ is $\chi^{\Phi} = s\bar{s}$.

In Refs. [15–19] a quark-diquark DA of the form ($c_1 = c_2 = 0$ for S diquarks)

$$\phi_D^B(x_1) = N^B x_1(1-x_1)^3(1 + c_1 x_1 + c_2 x_1^2) \times \exp\left[-b^2\left(\frac{m_q^2}{x_1} + \frac{m_D^2}{(1-x_1)}\right)\right] \quad (2.9)$$

turned out to be quite appropriate for octet baryons B. The origin of the phenomenological baryon DA, Eq. (2.9), is a non-relativistic harmonic-oscillator wave function (cf. Ref. [21]). Therefore the masses appearing in the exponential have to be considered as constituent masses (330 MeV for light quarks, 580 MeV for light diquarks; strange quarks are 150 MeV heavier than light quarks). The oscillator parameter $b^2 = 0.248\ \text{GeV}^{-2}$ is chosen in such a way that the full wave function gives rise to a value of 600 MeV for the mean intrinsic transverse momentum of quarks inside a nucleon. This value of the mean intrinsic transverse momentum is consistent with the one found by the EMC [22] in semi-inclusive deep inelastic μp scattering. The exponential in the baryon DA, Eq. (2.9), not only provides a flavor dependence, but also suppresses the end-point regions $x_1, y_1 \to 0, 1$ in the convolution integral, Eq. (2.1). One thus avoids to pick up sizable contributions from the soft end-point regions and results become less dependent on details of the baryon DA. In the actual data fitting the exponential plays only a minor role. Therefore, the constituent masses and the oscillator parameter have not been considered as free parameters but have been fixed in advance. We stress that the constituent masses do not appear in the hard scattering amplitudes (cf. Sec. II D below).

A model for the Φ meson DA which fulfills QCD sum-rule constraints has been proposed by Benayoun and Chernyak [23]. Since we also want to investigate to which extent our calculations for Φ production may be generalized to J/ψ production, we modify this DA by attaching an exponential factor which provides a flavor dependence. The effect of this factor is negligible for ϕ's, but it becomes crucial for J/ψ's. The form of the exponential factor is inspired by a simple relativistic treatment of heavy mesons [24] and provides a flavor dependence in accordance with heavy-quark effective theory. For longitudinally polarized ϕ's and J/ψ's the DA reads ($M = \Phi, J/\psi$)

$$\phi^M(z_1,\lambda_M = 0) = N^M_{\lambda_M=0} z_1(1-z_1)\exp[-\tilde{b}^2 m_M^2 (z_1 - 0.5)^2]. \quad (2.10)$$

The DA for transversally polarized ϕ's and J/Ψ's contains an additional polynomial in z_1 which enhances the maximum at $z_1 = 0.5$ and makes it narrower:

$$\phi^M(z_1,\lambda_M = \pm 1) = N^M_{\lambda_M=\pm 1} z_1(1-z_1) \times \exp[-\tilde{b}^2 m_M^2 (z_1 - 0.5)^2] \times [5225.2\, z_1^6 (1-z_1)^6 + 0.39\, z_1(1-z_1)]. \quad (2.11)$$

This form for the DA of transversally polarized Φ mesons has been introduced in Ref. [23] (apart from the exponential) to satisfy QCD sum-rule constraints on the lowest moments of $\phi^{\Phi}(z_1,\lambda_{\Phi} = \pm 1)$. In our present investigation, however, it is only relevant that this DA is narrower than the asymptotic one. Our numerical studies show that choosing instead $\phi^{\Phi}(z_1,\lambda_{\Phi} = \pm 1) \propto z_1^8(1-z_1)^8$ would change the results for differential cross sections and polarization observables by less than 5%. For the oscillator parameter $\tilde{b}$ we take a value of $0.97\ \text{GeV}^{-1}$ in accordance with estimates for the radius of the J/ψ meson [25].

The usual normalization condition, $\int_0^1 dx\, \phi^H(x) = 1$, fixes the constants N^B and $N^M_{\lambda_{\Phi}}$ in Eqs. (2.9), (2.10), and (2.11). The quantity f^M showing up in Eq. (2.8) is related to the experimentally determinable decay constant f^M_{decay} of the meson M. From the radiative decay width of the $\Phi \to e^+e^-$ decay one gets a value of $f^{\Phi}_{\text{decay}} = 237 \pm 4$ MeV [26], whereas from QCD sum rules one derives $f^{\Phi}_{\text{decay}} = 230$ MeV [23]. The latter gives $f^{\Phi} = f^{\Phi}_{\text{decay}}/2\sqrt{6} = 46.95$ MeV which we take for our calculations. The analogous constants f_S^B and f_V^B for the q-D DAs of baryon B are free parameters of the diquark model. They are, in principle, determined by the probability to find the q-D state ($D = S, V$) in the baryon B and by the transverse-momentum dependence of the corresponding wave function.

Our present study is performed with the set of diquark-model parameters found in Ref. [15] by fitting elastic electron-nucleon scattering data. The numerical values of the parameters are

$$f_S = 73.85\ \text{MeV}, \quad Q_S^2 = 3.22\ \text{GeV}^2, \quad a_S = 0.15,$$
$$f_V = 127.7\ \text{MeV}, \quad Q_V^2 = 1.50\ \text{GeV}^2, \quad a_V = 0.05,$$
$$\kappa_V = 1.39, \quad c_1 = 5.8, \quad c_2 = -12.5. \quad (2.12)$$

For further details of the diquark model we also refer to the paper of Jakob *et al.* [15].

B. General structure of the hard-scattering amplitude

The introduction of diquark form factors already requires a decomposition of the hard-scattering amplitude $\hat{T}_{\{\lambda\}}$ into 3- and 4-point contributions

$$\begin{aligned}\hat{T}_{\{\lambda\}}(x_1,y_1,z_1;\hat{s},\hat{t}) = {} & e_s \hat{T}^{(Q,S)}_{\{\lambda\}}(x_1,y_1,z_1;\hat{s},\hat{t}) \\ & + e_u \hat{T}^{(q,S)}_{\{\lambda\}}(x_1,y_1,z_1;\hat{s},\hat{t}) \\ & + e_{S_{[u,d]}} \hat{T}^{(S)}_{\{\lambda\}}(x_1,y_1,z_1;\hat{s},\hat{t}) \\ & + e_s \hat{T}^{(Q,V)}_{\{\lambda\}}(x_1,y_1,z_1;\hat{s},\hat{t}). \end{aligned} \tag{2.13}$$

e_q and $e_{S_{[u,d]}}$ are the electric charges of the quark q and the S diquark $S_{[u,d]}$ in units of e_0, respectively. The superscripts indicate whether the photon couples to the heavy quark Q in the meson or the light quark q in the proton with the diquark $D=S,V$ acting as spectator (3-point contributions), or whether the photon couples to the S or V diquark in the proton (4-point contributions). Note that the only V-diquark contribution is $\hat{T}^{(Q,V)}_{\{\lambda\}}$. The reason is that the charge-flavor factor in front of $\hat{T}^{(q,V)}_{\{\lambda\}}$ vanishes and $\hat{T}^{(V)}_{\{\lambda\}}$ represents already a mass correction of second order, which is neglected in our calculation. For the numerical treatment of the convolution integral, Eq. (2.1), it is advantageous to further split the n-point contributions into two parts which differ by their propagator singularities:

$$\begin{aligned}\hat{T}^{(Q,D)}_{\{\lambda\}}(x_1,y_1,z_1;\hat{s},\hat{t}) &= \left[\frac{f^{(Q,D)}_{\{\lambda\}}(x_1,y_1,z_1;\hat{s},\hat{t})}{(\hat{q}_2^2+i\epsilon)(\hat{q}_5^2+i\epsilon')} + \frac{g^{(Q,D)}_{\{\lambda\}}(x_1,y_1,z_1;\hat{s},\hat{t})}{(\hat{q}_3^2+i\epsilon)(\hat{q}_4^2+i\epsilon')}\right] F_D^{(3)}(-x_2y_2\hat{t}), \\ \hat{T}^{(q,D)}_{\{\lambda\}}(x_1,y_1,z_1;\hat{s},\hat{t}) &= \left[\frac{f^{(q,D)}_{\{\lambda\}}(x_1,y_1,z_1;\hat{s},\hat{t})}{(\hat{g}_1^2+i\epsilon)(\hat{q}_2^2+i\epsilon')} + \frac{g^{(q,D)}_{\{\lambda\}}(x_1,y_1,z_1;\hat{s},\hat{t})}{(\hat{g}_1^2+i\epsilon)(\hat{q}_3^2+i\epsilon')}\right] F_D^{(3)}(-x_2y_2\hat{t}), \\ \hat{T}^{(D)}_{\{\lambda\}}(x_1,y_1,z_1;\hat{s},\hat{t}) &= \left[\frac{f^{(D)}_{\{\lambda\}}(x_1,y_1,z_1;\hat{s},\hat{t})}{(\hat{g}_2^2+i\epsilon)(\hat{q}_5^2+i\epsilon')} + \frac{g^{(D)}_{\{\lambda\}}(x_1,y_1,z_1;\hat{s},\hat{t})}{(\hat{g}_2^2+i\epsilon)(\hat{q}_4^2+i\epsilon')}\right] F_D^{(4)}(-x_2y_2\hat{t}). \end{aligned} \tag{2.14}$$

The functions f and g correspond to gauge-invariant subgroups of the 16 Feynman diagrams which contribute to the hard-scattering amplitude $\hat{T}_{\{\lambda\}}$ (cf. Fig. 2). The diagrams entering the g's are related to those entering the f's by interchange of the two gluons. The q_i^{-2} and g_i^{-2} denote just those quark and gluon propagators which can go on shell when integrating over x_1, y_1, and z_1. Explicitly, the propagator denominators read

$$\begin{aligned}&\hat{q}_2^2 = y_2z_2\hat{s} + x_2y_2\hat{t} + x_2z_2\hat{u}, \quad \hat{q}_3^2 = y_2z_1\hat{s} + x_2y_2\hat{t} + x_2z_1\hat{u}, \\ &\hat{q}_4^2 = y_1z_2\hat{s} + x_1y_1\hat{t} + x_1z_2\hat{u}, \quad \hat{q}_5^2 = y_1z_1\hat{s} + x_1y_1\hat{t} + x_1z_1\hat{u}, \\ &\hat{g}_1^2 = x_1y_2\hat{s} + x_2y_1\hat{u}, \quad \hat{g}_2^2 = x_2y_1\hat{s} + x_1y_2\hat{u}. \end{aligned} \tag{2.15}$$

As already indicated in Eq. (2.14) propagator singularities are treated by means of the usual $i\epsilon$ prescription. The resulting imaginary part in the amplitudes is considered as a nontrivial prediction of perturbative QCD which is unaffected by long-distance effects [27]. As we will see below, it gives rise to non-vanishing predictions for polarization observables which require the flip of a hadronic helicity. For analytical expressions of the functions f and g and their symmetry properties we refer to Sec. III.

C. Numerical treatment of propagator singularities

The numerical difficulties in performing the convolution integral, Eq. (2.1), are mainly caused by the occurrence of propagator singularities in the range of the (x_1,y_1,z_1) integration. These give rise to principal value integrals

$$\frac{1}{k^2 \pm i\epsilon} = \wp\left(\frac{1}{k^2}\right) \pm i\pi\delta(k^2). \tag{2.16}$$

As explained in some detail in Ref. [19] such integrals can still be treated by means of a rather fast and stable fixed-point Gaussian quadrature after carefully separating the principal value parts and doing the corresponding integrations analytically. Here we only want to give a short account of our integration procedure. We first perform the x_1 integration for which the various contributions to the hard scattering amplitude [cf. Eq. (2.14)] lead to integrals of the general form

$$I^{(k_1,k_2)}(y_1,z_1) = \int_0^1 dx_1 \frac{h(x_1,y_1,z_1)}{(k_1^2+i\epsilon)(k_2^2+i\epsilon')}. \tag{2.17}$$

In order to simplify the notation we have neglected helicity labels and the dependence on the Mandelstam variables $\hat{s}$ and $\hat{t}$. Furthermore, the distribution amplitudes have been absorbed into the function $h(x_1,y_1,z_1)$. By applying a partial fractioning, exploiting Eq. (2.16), and separating the principal value part, Eq. (2.17) may be rewritten to give

$$I^{(k_1,k_2)}(y_1,z_1)=\frac{1}{x_1^{(k_1)}-x_1^{(k_2)}+i\tilde{\epsilon}}\left\{\left(\frac{\partial k_2^2}{\partial x_1}\right)^{-1}\int_0^1 dx_1\,\frac{h(x_1,y_1,z_1)-h(x_1^{(k_1)},y_1,z_1)}{k_1^2}\right.$$
$$\left.+\left(\frac{\partial k_2^2}{\partial x_1}\right)^{-1}h(x_1^{(k_1)},y_1,z_1)\left(\wp\int_0^1\frac{dx_1}{k_1^2}-i\pi\left|\frac{\partial k_1^2}{\partial x_1}\right|^{-1}\right)-\text{same}\,(k_1\leftrightarrow k_2)\right\}. \tag{2.18}$$

$x_1^{(k_1)}=x_1^{(k_1)}(y_1,z_1)$ and $x_1^{(k_2)}=x_1^{(k_2)}(y_1,z_1)$ are the zeros of the propagator denominators k_1^2 and k_2^2, respectively, and $\tilde{\epsilon}$ stands for either ϵ or ϵ', depending for which of the two the limit $\epsilon^{(\prime)}\to 0$ has been taken. As long as the two zeros $x_1^{(k_1)}$ and $x_1^{(k_2)}$ (which still depend on y_1 and z_1) do not coincide in the (y_1,z_1)-integration region—this is the case for the contributions of $f^{(q,D)}$, $g^{(q,D)}$, $f^{(D)}$, and $g^{(D)}$—the (x_1,y_1,z_1) integration can be performed very efficiently with the help of Eq. (2.18). After analytic integration of the two principal-value integrals in Eq. (2.18) (which is a simple matter) all the integrands of the remaining integrations are regular functions of the integration variables and can be treated by fixed-point Gaussian quadrature.

For $f^{(Q,D)}$ and $g^{(Q,D)}$, however, the situation becomes a little bit more complicated. After having performed the x_1 integration in Eq. (2.18) one observes that the two propagator singularities $x_1^{(k_1)}$ and $x_1^{(k_2)}$ coincide along a trajectory in the (y_1,z_1)-integration region. This leads to a quadratic zero $y_1^{(k_1,k_2)}=y_1^{(k_1,k_2)}(z_1)$ of $(x_1^{(k_1)}-x_1^{(k_2)})$. A closer inspection of Eq. (2.18) reveals that this quadratic zero in the denominator of $I^{(k_1,k_2)}(y_1,z_1)$ does not cause any further problem when performing the (y_1,z_1) integration for the real part of $I^{(k_1,k_2)}(y_1,z_1)$. The reason is that it is completely compensated by a corresponding quadratic zero in the numerator of $\Re I^{(k_1,k_2)}(y_1,z_1)$. In $\Im I^{(k_1,k_2)}(y_1,z_1)$, however, the zero of $(x_1^{(k_1)}-x_1^{(k_2)})$ is only partly compensated by the numerator and one still encounters a single pole. At the pole $\Im I^{(k_1,k_2)}(y_1,z_1)$ becomes proportional to $(y_1-y_1^{(k_1,k_2)})/[(y_1-y_1^{(k_1,k_2)})^2+i\tilde{\epsilon}]=\{1/(y_1-y_1^{(k_1,k_2)}+i\hat{\epsilon})+1/(y_1-y_1^{(k_1,k_2)}-i\hat{\epsilon})\}/2$. As a consequence $\int_0^1 dy_1\Im I^{(k_1,k_2)}(y_1,z_1)$ becomes a pure principal-value integral [cf. Eq. (2.16)]:

$$\int_0^1 dy_1\Im I^{(k_1,k_2)}(y_1,z_1)=\wp\int_0^1 dy_1\Im I^{(k_1,k_2)}(y_1,z_1), \tag{2.19}$$

which can be treated numerically analogous to the principal-value integral in x_1. One only has to separate the principal-value part and do the corresponding integration analytically. For this purpose the analytical expression of the residue of $\Im I^{(k_1,k_2)}(y_1,z_1)$ at the position of the pole $y_1^{(k_1,k_2)}(z_1)$ is needed. The remaining integrations are then again amenable to Gaussian quadrature.

Thus it is possible, by carefully separating the singular contributions, exploiting δ functions, rewriting principal-value integrals as ordinary integrals plus analytically solvable principal-value integrals, to do all the numerical integrations by means of fixed-point Gaussian quadrature. Whereas the authors of Ref. [28], who have used a different integration procedure, were only able to obtain reliable results for the imaginary part of the convolution integral, Eq. (2.1), our numerical results for the imaginary *and* real parts turn out to be very stable. Going from an $x_1\times y_1\times z_1$ grid of $24\times 24\times 20$ points to a $48\times 48\times 32$ grid changes the results for the amplitudes (over the whole angular range) by less than 0.1%. Our numerical calculations were performed on an AlphaServer 1000 4/266. For the larger grid size the evaluation of $d\sigma/dt(\gamma p\to\Phi p)$ (taking into account the 8 hadronic non- and single-flip amplitudes) took less than 7 sec per energy point and angle.

D. Treatment of mass effects

Our calculation of the hard-scattering amplitude involves an expansion in powers of $(m_H/\sqrt{\hat{s}})$ which is performed at fixed scattering angle. We keep only the leading order and next-to-leading order terms in this expansion. Hadron masses, however, are fully taken into account in flux and phase-space factors. The reasons why we want to include hadron-mass effects in the hard scattering amplitude are twofold. On the one hand, we want to apply our model already at momentum transfers of only a few GeV, where hadron masses may still play a role. On the other hand, we also want to make predictions for spin observables which require the flip of hadronic helicities. Within usual perturbative QCD such observables would vanish since a spin-1 gauge boson which couples to a nearly massless (current) quark cannot flip the helicity of the quark. In the original diquark model [15] violations of hadronic helicity conservation are generated by massive V diquarks on the account of introducing a mass parameter for the V diquark. In this paper we adopt another strategy which allows for a more consistent treatment of mass effects without introducing new mass parameters for the hadronic constituents. Like the authors of Ref. [29] we assume for every hadronic constituent that its 4-momentum is proportional to the 4-momentum of its parent hadron. This requires us to assign to every constituent of the hadron H an effective mass xm_H, where x is the fraction of the four-momentum of the hadron H carried by the constituent. Keeping in mind that the momentum fractions are weighted by the hadron DAs in the convolution integral, Eq. (2.1), this means that quarks and diquarks acquire (on the average) a mass which is rather the mass of a constituent than a current particle. This may be interpreted in such a way

that at intermediate momentum transfers a quark or diquark surrounded by a cloud of $q\bar{q}$ pairs and gluons is not resolved but rather acts like a single effective particle with a corresponding mass.

This prescription for the constituent masses applies to the (on-shell) particles which correspond to the external legs of the Feynman diagrams. It has already been tacitly exploited when casting the hadronic spin wave functions into covariant form [cf. Eqs. (2.6) and (2.8)]. Taking the quark-diquark DA of Eq. (2.9) the average values of the effective masses of quarks and diquarks in a proton become

$$\langle m_q^{\rm eff}\rangle = \langle x_1\rangle m_p \approx \frac{1}{3} m_p ,$$

$$\langle m_D^{\rm eff}\rangle = \langle (1-x_1)\rangle m_p \approx \frac{2}{3} m_p . \tag{2.20}$$

Analogously the effective mass of the heavy (anti)quark in the meson becomes on the average half of the meson mass. The choice of the masses which occur in the propagators of internal particles is not that obvious, since, e.g., a quark in the incoming proton has mass $x_1 m_p$ whereas the same quark in the outgoing proton has mass $y_1 m_p$. So what should we take for the mass of this quark between two vertices? In order to explain our recipe we, e.g., consider the momentum of the heavy quark between the two gluon vertices in the third diagram of Fig. 2. It is

$$q_5 = z_1 k + y_1 p_f - x_1 p_i , \tag{2.21}$$

with p_i, p_f and k representing the 4-momenta of the hadrons as indicated in Fig. 1. The quark mass in the propagator related to q_5 is now obtained by replacing the 4-momenta in Eq. (2.21) by the masses of the corresponding particles, i.e.

$$m_Q^{(q_5)} = z_1 m_M + (y_1 - x_1) m_p . \tag{2.22}$$

Taking again into account that the momentum fractions are weighted by the hadron DAs, Eq. (2.9) and Eq. (2.10), the average heavy quark mass in the propagator becomes $\langle m_Q^{(q_5)}\rangle \approx 0.5\, m_M$. Extending this recipe to all the quark and diquark propagators and using the covariant wave-function representations, Eqs. (2.6) and (2.8), for the external particles, leads to analytical expressions for the Feynman diagrams which contain (apart of the momentum fractions x_i, y_i, and z_i) only hadronic momenta, masses, spinors, polarization vectors, and helicities. The occurring traces and spinor products can be evaluated in the usual way. The final step is then to reexpress the (massive) Mandelstam variables s, t, and u in terms of massless ones

$$\begin{aligned} s &= \hat{s}[1+\mathcal{O}(m_H^2/\hat{s})] \quad \text{with} \quad \hat{s} = 4q^2, \\ t &= \hat{t}[1+\mathcal{O}(m_H^2/\hat{s})] \quad \text{with} \quad \hat{t} = -2q^2[1-\cos(\theta_{\rm c.m.})], \\ u &= \hat{u}[1+\mathcal{O}(m_H^2/\hat{s})] \quad \text{with} \quad \hat{u} = -2q^2[1+\cos(\theta_{\rm c.m.})], \end{aligned} \tag{2.23}$$

and to make an expansion in terms of the (small) parameters $(m_H/\sqrt{\hat{s}})$, keeping the scattering angle $\theta_{\rm c.m.}$ fixed. In order to facilitate the treatment of propagator singularities we retain only the leading and next-to-leading order terms in this expansion. Taking again as an example the propagator related to the momentum q_5 [cf. Eq. (2.21)] the propagator denominator becomes

$$\begin{aligned} (q_5^2 - m_Q^{(q_5)2}) &= y_1 z_1 [s - (m_p + m_M)^2] + x_1 y_1 t + x_1 z_1 [u - (m_p - m_M)^2] \\ &= y_1 z_1 \hat{s}[1+\mathcal{O}(m_H^2/\hat{s})] + x_1 y_1 \hat{t}[1+\mathcal{O}(m_H^2/\hat{s})] + x_1 z_1 \hat{u}[1+\mathcal{O}(m_H^2/\hat{s})] \approx \hat{q}_5^2, \end{aligned} \tag{2.24}$$

hence the quark propagator is given by

$$\frac{\not{q}_5 + m_Q^{(q_5)}}{\hat{q}_5^2 + i\epsilon} . \tag{2.25}$$

I.e., by neglecting mass corrections of $\mathcal{O}(m_H^2/\hat{s})$ we end up with propagator denominators which still appear like those of massless particles [cf. Eq. (2.15)]. Apart from the simplifications in the treatment of propagator singularities and in the analytical expressions for the hard part of the amplitudes our approximate treatment of mass effects has a few other nice features. By including mass corrections of $\mathcal{O}(m_H/\sqrt{\hat{s}})$ we obtain non-vanishing results for hadron-helicity-flip amplitudes and thus for polarization observables which require the flip of a hadronic helicity (see the discussion in the next section). Like the leading-order hadron-helicity-conserving amplitudes also the hadron-helicity-flip amplitudes are $U(1)$ gauge invariant with respect to the photon and $SU(3)$ gauge invariant with respect to the gluon. Finally, crossing relations for the hadronic helicity amplitudes are fulfilled up to $\mathcal{O}(m_H/\sqrt{\hat{s}})$, as has been shown for Compton scattering off baryons and its crossed process $\gamma\gamma \to B\bar{B}$ [18].

III. HELICITY AMPLITUDES AND OBSERVABLES

For exclusive photoproduction of vector mesons $\gamma p \to M p$ one finds, altogether, 24 complex helicity amplitudes. By virtue of parity invariance only 12 of these helicity amplitudes are independent. Following the notation of Ref. [30] we denote them by

$$H_{1,\lambda_\Phi} = M_{\lambda_\Phi,\lambda_f=+1/2,\lambda_\gamma=1,\lambda_i=-1/2},$$
$$H_{2,\lambda_\Phi} = M_{\lambda_\Phi,\lambda_f=+1/2,\lambda_\gamma=1,\lambda_i=+1/2},$$
$$H_{3,\lambda_\Phi} = M_{\lambda_\Phi,\lambda_f=-1/2,\lambda_\gamma=1,\lambda_i=-1/2},$$
$$H_{4,\lambda_\Phi} = M_{\lambda_\Phi,\lambda_f=-1/2,\lambda_\gamma=1,\lambda_i=+1/2}, \tag{3.1}$$

with $\lambda_\Phi = 0, \pm 1$. For our normalization of the helicity amplitudes the unpolarized differential cross section takes on the form

$$\frac{d\sigma}{dt} = \frac{1}{32\pi(s-m_p^2)^2} \sum_{\lambda_\Phi=0,\pm1} \sum_{i=1}^{4} |H_{i,\lambda_\Phi}|^2. \tag{3.2}$$

As examples for single spin observables, for which our model provides nontrivial predictions, we will consider the beam and target asymmetry. The corresponding expressions are [30]

$$\Sigma_x \frac{d\sigma}{dt} = \frac{d\sigma_\parallel}{dt} - \frac{d\sigma_\perp}{dt} = -\frac{1}{16\pi(s-m_p^2)^2} \Re(H^*_{4,1}H_{1,-1} - H^*_{4,0}H_{1,0} + H^*_{4,-1}H_{1,1} - H^*_{3,1}H_{2,-1} + H^*_{3,0}H_{2,0} - H^*_{3,-1}H_{2,1}) \tag{3.3}$$

for the photon and

$$\mathcal{T}_y \frac{d\sigma}{dt} = -\frac{1}{16\pi(s-m_p^2)^2} \Im(H^*_{4,-1}H_{3,-1} + H^*_{4,0}H_{3,0} + H^*_{4,1}H_{3,1} + H^*_{2,-1}H_{1,-1} + H^*_{2,0}H_{1,0} + H^*_{2,1}H_{1,1}) \tag{3.4}$$

for the proton, respectively.

In photoproduction of vector mesons experimentalists often extract the vector meson's spin-density matrix elements from its decay distribution. These studies are simplest and yield most direct information in one of the rest frames of the decaying vector meson. If one chooses the (s-channel) helicity rest frame of the vector meson and considers unpolarized photons and protons, this density matrix is easily expressed in terms of our helicity amplitudes in the γp c.m. system:

$$\rho^0_{\lambda_\phi\lambda'_\phi} = \frac{\sum_{\lambda_f,\lambda_\gamma,\lambda_i} M_{\lambda_\Phi,\lambda_f,\lambda_\gamma,\lambda_i} M^*_{\lambda'_\Phi,\lambda_f,\lambda_\gamma,\lambda_i}}{\sum_{\tilde{\lambda}_\Phi,\lambda_f,\lambda_\gamma,\lambda_i} |M_{\tilde{\lambda}_\Phi,\lambda_f,\lambda_\gamma,\lambda_i}|^2}. \tag{3.5}$$

For the connection between density matrices in the most commonly used rest frames (helicity, Gottfried-Jackson, Adair and transversity frame) and the definition of these frames we refer to Ref. [31].

Within the hard scattering approach the energy dependence of the helicity amplitudes at fixed c.m. angle and large s is roughly

$$H_{2,0}, H_{3,0} \propto s^{-5/2},$$
$$H_{1,0}, H_{4,0}, H_{2,1}, H_{3,1}, H_{2,-1}, H_{3,-1} \propto s^{-3},$$
$$H_{1,1}, H_{4,1}, H_{1,-1}, H_{4,-1} \propto s^{-7/2}, \tag{3.6}$$

depending on whether the helicity of the hadronic constituents is conserved or flipped by one or two units. This scaling behavior is modified by logarithms due to the running coupling α_s and, eventually, the evolution of the hadron distribution amplitudes. Further deviations are due to the diquark form factors. For small momentum transfers diquarks appear nearly point like and the decay behavior of the helicity amplitudes is weakened by one power of s. The energy dependence in Eqs. (3.6) is only approached at large enough momentum transfer, where the diquark form factors become fully operational.

For the helicity amplitudes our treatment of mass effects (cf. Sec. II D) leads to an expansion in powers of $(m_H/\sqrt{\hat{s}})^2$. As compared to the hadron-helicity-conserving amplitudes $H_{2,0}$ and $H_{3,0}$, the leading-order term of the single-flip amplitudes $H_{1,0}$, $H_{4,0}$, $H_{2,\pm1}$, and $H_{3,\pm1}$ is suppressed by $\mathcal{O}(m_H/\sqrt{\hat{s}})$. The leading-order term of the double-flip amplitudes $H_{1,\pm1}$ and $H_{4,\pm1}$ is even suppressed by $(m_H/\sqrt{\hat{s}})^2$ and thus has the same order as the first (non-vanishing) mass-correction term of the hadron-helicity-conserving amplitudes. To simplify matters we only consider non- and single-flip amplitudes to leading-order and neglect double-flip amplitudes at all.

In the following we quote the analytical results for the functions f and g which have been obtained with the help of the symbolic computer program ''MATHEMATICA,'' in particular with the two program packages ''FEYNARTS'' [32] and ''FEYNCALC'' [33]. In case of the hadron-helicity conserving amplitude $H_{3,0}$, i.e. for the helicity combination $\lambda_\Phi = 0$, $\lambda_f = -1/2$, $\lambda_\gamma = +1$, $\lambda_i = -1/2$, the functions f read

$$f^{(Q,S)}_{\{0,-1/2;+1,-1/2\}} = -\frac{6m_p^2}{\kappa\hat{t}} f^{(Q,V)}_{\{0,-1/2;+1,-1/2\}}$$

$$= -2V\frac{\hat{u}}{x_1x_2y_1y_2z_1z_2\hat{t}^3}((z_2-z_1)\{z_1z_2\hat{u}^2[x_1(1+x_2)-y_1(1+y_2)]+\hat{t}\hat{u}(x_2+y_2)(x_1-z_1)(y_1z_2+y_2z_1)$$

$$-y_2z_1^2\hat{t}^2(1+y_2)\}+x_1y_2\hat{t}^2[4z_1^2(y_1-z_1)+y_1(x_2+z_2)+z_1(2x_1z_1-3y_1)]), \tag{3.7a}$$

$$f^{(q,S)}_{\{0,-1/2;+1,-1/2\}} = -\frac{6m_p^2}{\kappa\hat{t}} f^{(q,V)}_{\{0,-1/2;+1,-1/2\}} = -4V\frac{1}{x_2y_1\hat{t}}\{x_2z_1\hat{u}+y_2z_2\hat{s}\}, \tag{3.7b}$$

$$f^{(S)}_{\{0,-1/2;+1,-1/2\}} = -4V\frac{1}{x_1y_1\hat{t}}\{x_1z_1\hat{u}+y_1z_2\hat{s}\}, \tag{3.7c}$$

with

$$V = 32\pi^2\sqrt{\pi\alpha}\,\alpha_s^2(\hat{t}\hat{u}/\hat{s})\sqrt{-\hat{t}}\,C_F, \tag{3.8}$$

where $C_F = 2/3\sqrt{3}$ denotes the color factor and α the fine-structure constant, respectively. The functions g are related to the f's in a simple way:

$$g^{(Q,D)}_{\{0,-1/2;+1,-1/2\}} = f^{(Q,D)}_{\{0,-1/2;+1,-1/2\}} \quad (z_1 \leftrightarrow z_2), \tag{3.9a}$$

$$g^{(q,D)}_{\{0,-1/2;+1,-1/2\}} = -f^{(q,D)}_{\{0,-1/2;+1,-1/2\}} \quad (z_1 \leftrightarrow z_2), \tag{3.9b}$$

$$g^{(S)}_{\{0,-1/2;+1,-1/2\}} = -f^{(S)}_{\{0,-1/2;+1,-1/2\}} \quad (z_1 \leftrightarrow z_2). \tag{3.9c}$$

Vector 4-point contributions $f^{(V)}$ and $g^{(V)}$ are, in general (for all helicity combinations), suppressed by $\mathcal{O}(m_H^2/\hat{s})$ or even stronger. Relations analogous to Eqs. (3.9) are also valid between the f's and g's entering the other $\lambda_\Phi = 0$ amplitudes $H_{1,0}$, $H_{2,0}$, and $H_{4,0}$. The functions f contributing to $H_{2,0}$—the other hadron-helicity conserving amplitude (helicity combination $\lambda_\Phi = 0$, $\lambda_f = +1/2$, $\lambda_\gamma = +1$, $\lambda_i = +1/2$)—are obtained from those entering $H_{3,0}$ by interchange of the Mandelstam variables $\hat{s} \leftrightarrow \hat{u}$ and the momentum fractions $x_1 \leftrightarrow y_1$:

$$f^{(Q,D)}_{\{0,+1/2;+1,+1/2\}} = f^{(Q,D)}_{\{0,-1/2;+1,-1/2\}} \quad (\hat{s} \leftrightarrow \hat{u}, x_1 \leftrightarrow y_1), \tag{3.10a}$$

$$f^{(q,D)}_{\{0,+1/2;+1,+1/2\}} = -f^{(q,D)}_{\{0,-1/2;+1,-1/2\}} \quad (\hat{s} \leftrightarrow \hat{u}, x_1 \leftrightarrow y_1), \tag{3.10b}$$

$$f^{(S)}_{\{0,+1/2;+1,+1/2\}} = -f^{(S)}_{\{0,-1/2;+1,-1/2\}} \quad (\hat{s} \leftrightarrow \hat{u}, x_1 \leftrightarrow y_1). \tag{3.10c}$$

The analytical expressions for the hadron-helicity-flip amplitudes $H_{1,0}$, $H_{4,0}$, $H_{2,\pm1}$, and $H_{3,\pm1}$ are of similar length as the expressions quoted above and can be obtained from the authors on request. Like in Eqs. (3.7) the vector 3-point contributions to $H_{2,\pm1}$ and $H_{3,\pm1}$ are proportional to the corresponding scalar ones. It is also interesting to observe that due to the (anti)symmetry properties of the Feynman graphs under interchange of the momentum fractions z_1 and z_2 [cf. Eqs. (3.9)], only diagrams in which the photon couples to the s quark contribute to the $\lambda_\Phi = 0$ amplitudes.

Actually we have computed all the functions f and g, and relations like Eqs. (3.9) and (3.10) served as a check of our analytical expressions. Furthermore, we have verified $U(1)$ gauge invariance with respect to the photon and $SU(3)$ gauge invariance with respect to the gluon. The proof of gauge invariance is facilitated by the observation that not only the sum of all 16 tree diagrams provides a gauge invariant expression, but rather each of the functions f and g is gauge invariant by itself. Finally, we have recalculated a few of the diagrams by hand to confirm the outcome of MATHEMATICA.

IV. NUMERICAL RESULTS

Figure 3 shows the diquark model predictions (solid line) for $d\sigma/dt[\gamma p \to \Phi p]$ at $p^\gamma_{\rm lab} = 6$ GeV together with the outcome of the Pomeron-exchange mechanism (dotted line) [4] and results of a two-gluon-exchange model (dash-dotted and dashed line) [34,35]. A direct comparison of our predictions with experiment is not possible yet since data are only available at low momentum transfers ($t \lesssim 1.5$ GeV^2) where the perturbative photoproduction mechanism is certainly not the dominant one. The experimental situation, however, will hopefully improve as soon as the data analysis of the CEBAF-93-031 experiment will be completed. Nevertheless, Fig. 3 shows that the diquark model provides a reasonable extrapolation of the low-t data. Thereby one should keep in mind that the cross section which decays exponentially in forward direction is expected to flatten around 90° (t and u large). The few available data for photoproduction of pseudoscalar mesons and also photoproduction of ρ and ω mesons which extend to larger values of t exhibit just such a

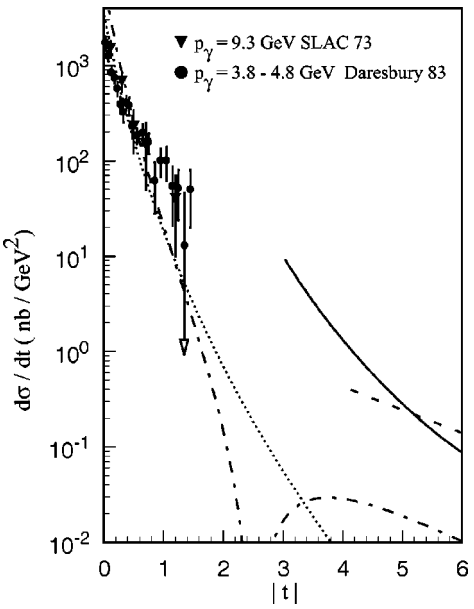

FIG. 3. Differential cross section for $\gamma p \to \Phi p$ versus t at $p^{\gamma}_{\rm lab} = 6$ GeV. The solid line corresponds to the diquark-model prediction. Cross sections resulting from the Pomeron-exchange mechanism [4] (dotted line) and a two-gluon-exchange model [34] (dash-dotted line) are plotted for comparison. The dashed line represents an attempt to extend the two-gluon-exchange model by including contributions in which the two gluons couple to different quarks inside the proton [35]. Data are taken from Ballam *et al.* [36] and Barber *et al.* [37].

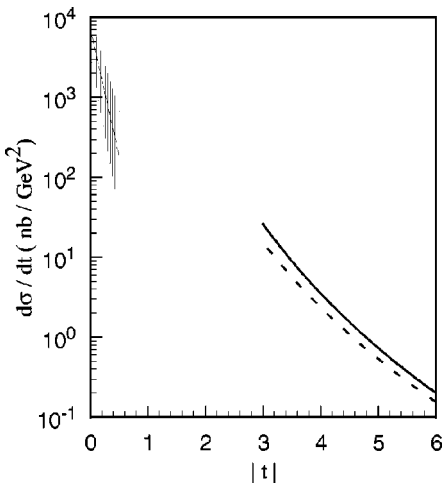

FIG. 4. Differential cross section for $\gamma p \to \Phi p$ versus t at $p^{\gamma}_{\rm lab} = 2611$ GeV ($s = 4900$ GeV^2). The diquark-model prediction with (solid line) and without (dashed line) mass effects is compared with a parametrization of the low-t ZEUS-data [39]. The hatched area indicates the uncertainties in the forward cross section and the slope parameter.

behavior [38]. As can be seen from Fig. 3 the forward cross section for ϕ production is reasonably well reproduced by simple Pomeron phenomenology (dotted line). As a mechanism for photoproduction of vector mesons Donnachie and Landshoff [4] proposed that the photon fluctuates into a quark-antiquark pair which subsequently recombines to a vector meson. The resulting quark loop is connected to a quark in the proton via the exchange of a single Pomeron which couples to quarks like an isoscalar photon. The QCD-inspired version of the Pomeron exchange of Donnachie and Landshoff [5], in which the Pomeron is replaced by two non-perturbative (Abelian) gluons, has been applied by Laget and Mendez-Galain [34] to photoproduction of Φ mesons (dash-dotted line). The latter authors consider the two-gluon-exchange model as a link which connects the diffractive with the hard-scattering domain. At $t \approx 2.5$ GeV^2 the two-gluon-exchange cross section exhibits a characteristic node which can be understood as an interference effect between the two Feynman diagrams which enter the photoproduction amplitude. However, this picture changes drastically if the two gluons are allowed to couple to different quarks in the proton. Recently Laget [35] tried to estimate such contributions by modeling quark-quark correlations inside a proton via a simple wave function. He found that the node in the cross section is completely washed out and that the contributions in which the two gluons couple to different quarks inside the proton start to dominate the photoproduction of Φ with increasing t (dashed line). Actually, for $|t| \gtrsim 4$ GeV^2 the result of Laget becomes comparable with the diquark-model result. This is not surprising since we know from the perturbative analysis that the hard-scattering mechanism, i.e. contributions from diagrams without loops in which all the hadronic constituents are connected via gluon exchange, should become dominant for large values of t and u. Correlations between hadronic constituents are automatically accounted for within such an approach and hence also within our diquark model.

To check whether our model provides a reasonable energy dependence we have also calculated the differential cross section at a much larger photon energy ($p^{\gamma}_{\rm lab} = 2611$ GeV). The result is depicted in Fig. 4 (solid line) along with a two-parameter fit of $|t| \leqslant 0.5$ GeV^2 data from ZEUS [39]. The hatched area indicates the uncertainties in the forward cross section and the slope parameter. Keeping again in mind that the cross section is expected to flatten with increasing t the magnitude of our prediction occurs still to be within the range of an extrapolation of the low-t data. The dashed line in Fig. 4 represents a leading-order calculation in which mass effects are neglected. This means that only the two hadron-helicity conserving amplitudes $H_{2,0}$ and $H_{3,0}$ are taken into account in the leading-order cross section. A comparison between the full calculation (solid line) and the leading-order calculation (dashed line) reveals that mass effects are still sizable and amount to ≈ 25–$40\,\%$ of the full differential cross section. They increase in forward and backward direction and are smallest around 90°.

At this point we want to comment on another attempt to calculate photoproduction of Φ mesons within the diquark model. The authors of Ref. [28] use a different parametrization of the model. Only the hadron-helicity-conserving amplitudes $H_{2,0}$ and $H_{3,0}$ are taken into account in their calculation. With their numerical method they encounter difficulties in calculating the real parts of these amplitudes. But they assert that the real parts are small for their parametrization and therefore neglect them. Their results for differ-

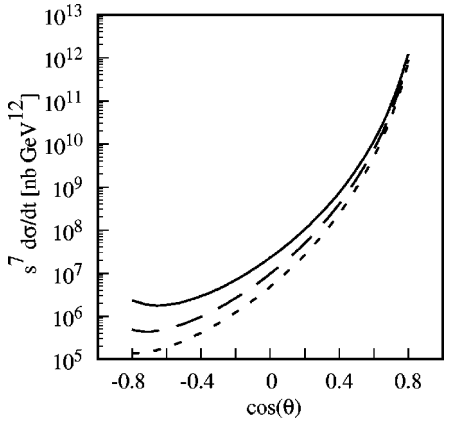

FIG. 5. Differential cross section for $\gamma p \to \Phi p$ scaled by s^7 versus $\cos(\theta_{\text{c.m.}})$. Diquark-model results for $p^{\gamma}_{\text{lab}}=5$ (solid line), 10 (long-dashed line), and 20 GeV (dashed line).

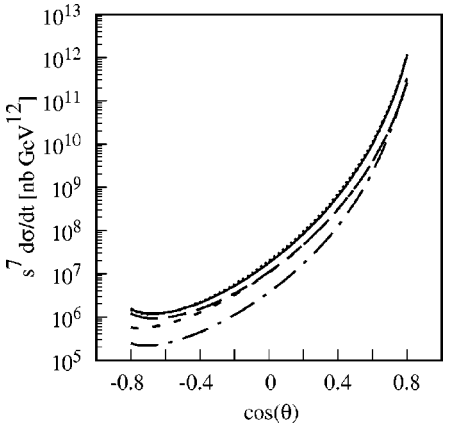

FIG. 6. Differential cross section for $\gamma p \to \Phi p$ scaled by s^7 versus $\cos(\theta_{\text{c.m.}})$ at $p^{\gamma}_{\text{lab}}=6$ GeV. A comparison of different contributions within the diquark model: full calculation (solid line), mass effects neglected (short-dashed line), *S* diquarks only (dash-dotted line), longitudinally polarized Φ's only (long-dashed line), exponential in Φ-DA neglected (dotted line).

ential cross sections are about one order of magnitude smaller than ours. This is plausible if one looks at their values of f_S^p and f_V^p, i.e. the ''normalization'' of the quark-diquark DAs and the cutoff masses in the diquark form factors. Both are considerably smaller than ours. In contrast to the authors of Ref. [28] we think that the present experimental situation in Φ photoproduction does not allow to discriminate a particular parametrization of the diquark model. However, we want to point out that our parametrization has already been applied successfully to a variety of other exclusive processes [15–19]. On the other hand, it is still unclear whether these processes can also be described satisfactorily with the parametrization of Carimalo *et al.* [28]. Their parameterization has been determined by means of the proton magnetic form factor. Apart from Φ photoproduction it has only been applied to charmonium decays into the $p\bar{p}\gamma$ final state [40] with the result that the data could not be reproduced.

In the kinematic region, where *t* and *u* are large, the differential cross section at fixed scattering angle is expected to exhibit a scaling behavior of approximately s^{-7}, which is supposed to indicate that the hard photoproduction mechanism becomes relevant. Figure 5 shows $s^7\, d\sigma/dt$ for photon energies of $p^{\gamma}_{\text{lab}}=5$, 10, and 20 GeV. Here 5 GeV is presently the upper limit of CEBAF, 10 GeV will be reached by the planned upgrade of CEBAF and 20 GeV is a value which could be reached at future facilities like ELFE or a further extension of CEBAF which are presently still under discussion. Comparing the diquark-model results for these energies one observes that one is still far away from the s^{-7} scaling behavior. The reasons have already been mentioned in Sec. III. A closer inspection shows that the cross section at $\theta_{\text{c.m.}}=90°$ scales rather like s^{-8} than s^{-7} for $10<s<40$ GeV. Starting with point-like diquarks and a constant α_s one would expect that the leading-order cross section (without mass effects) should scale like s^{-5}. By including the diquark form factors and cross-section contributions from hadron-helicity-flip amplitudes, which are already suppressed by one power of *s* as compared to the leading-order contributions, the scaling behavior changes already to nearly s^{-7}. Finally, the approximate s^{-8} decay is caused by the fact that α_s is taken as a running coupling constant [with argument $(\hat{t}\hat{u}/\hat{s})$].

Figure 6 shows how the differential cross section (at $p^{\gamma}_{\text{lab}}=6$ GeV) is influenced by different contributions within our model. A comparison of the solid (full calculation) and the short-dashed (mass effects neglected) line reveals, e.g., the influence of mass effects. For $p^{\gamma}_{\text{lab}}=6$ GeV and $\cos(\theta_{\text{c.m.}})=90°$ they amount to $\approx 40\%$ of the full cross section. The dash-dotted line represents the pure *S*-diquark part of the cross section. It varies between 15% and 30% if one goes from backward to forward angles. Since *S*- and *V*-diquark contributions add coherently [and constructively; cf. Eq. (3.7)] this means that the corresponding amplitudes are of the same order of magnitude. The differential cross section for the photoproduction of longitudinally polarized Φ's is given by the long-dashed curve. It amounts to $\approx 60\%$ of the full cross section at $\cos(\theta_{\text{c.m.}})=90°$. This fraction increases in backward direction and decreases in forward direction. In addition we have examined the influence of the exponential in the Φ DA [cf. Eq. (2.10)]. Neglecting this exponential one ends up with the dotted curve which is nearly indistinguishable from the full calculation. This also shows that we are not very sensitive to the $z_1 \to 0,1$ end-point regions when performing the convolution integral Eq. (2.1). Finally, we have also checked whether a particular group of Feynman graphs contributes predominantly to cross sections and polarization observables. Our finding is that those graphs in which the photon couples to the strange quark in the Φ meson are by far the most important. The fraction of their contribution to unpolarized differential cross sections is more than 95% and still more than 70% in the polarization observables we have considered.

As examples for single-polarization observables the beam asymmetry Σ_x and the target asymmetry $\mathcal{T}_y$ are depicted in Fig. 7. The beam asymmetry would be already non-zero, if only the leading-order helicity amplitudes $H_{2,0}$ and $H_{3,0}$ were

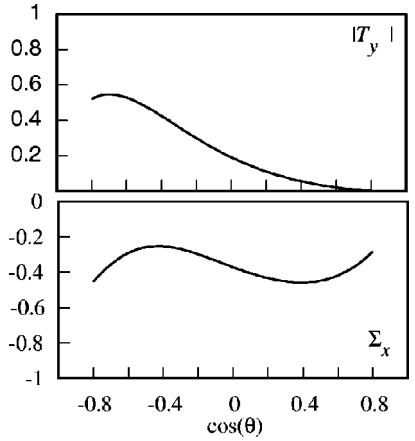

FIG. 7. Diquark-model predictions for beam (Σ_x) and target ($\mathcal{T}_y$) asymmetry in $\gamma p \to \Phi p$ scattering at $p^{\gamma}_{\rm lab}=6$ GeV.

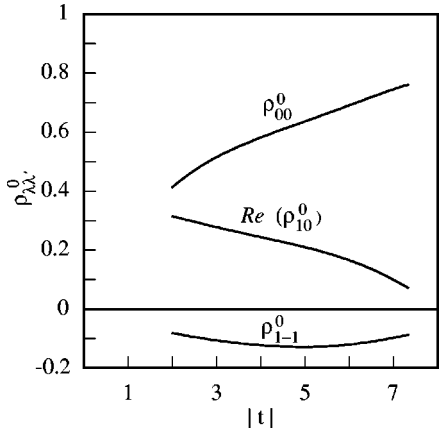

FIG. 8. Diquark-model predictions for the Φ spin-density matrix elements in the *s*-channel helicity frame for $\gamma p \to \Phi p$ scattering at $p^{\gamma}_{\rm lab}=6$ GeV.

taken into account [cf. Eq. (3.3)]. It would not even be necessary that the helicity amplitudes acquire a non-trivial phase. On the other hand, a non-trivial target asymmetry demands for non-vanishing hadron-helicity-flip amplitudes as well as for non-trivial phases of the amplitudes [cf. Eq. (3.4)]. As already mentioned at the end of Sec. II B phases are generated through propagator singularities, and hadron-helicity-flip amplitudes occur in our model as mass corrections. As it turns out within our model, also the beam asymmetry is considerably affected by the inclusion of the hadron-helicity-flip amplitudes. In a recent paper [41] the influence of nucleonic resonance effects on polarization observables in Φ-meson photoproduction has been investigated within a constituent-quark model in which the diffractive contribution is produced by *t*-channel Pomeron exchange. It is interesting to observe that the result of these authors for the target asymmetry at a rather small photon energy of $p^{\gamma}_{\rm lab}=2$ GeV is comparable in size to our result at $p^{\gamma}_{\rm lab}=6$ GeV. This is remarkable since two completely different concepts are at work: on the one hand nucleonic resonance contributions, on the other hand a purely perturbative mechanism. Also for the beam asymmetry some similarities can be found. The corresponding predictions of both approaches are again comparable around $\theta_{\rm c.m.}=90°$. A (somewhat smaller) negative beam asymmetry has also been found in another model which is based on Pomeron exchange, pion exchange, and a direct knockout production from the strange-quark sea in the proton [42]. It would be interesting to see experimentally, whether polarization observables like the target asymmetry $\mathcal{T}_y$, the recoil polarization $\mathcal{P}_{y'}$, or the vector-meson polarization $\mathcal{V}_{y'}$, which vanish in leading-order perturbative QCD, are still sizable at momentum transfers of a few GeV. Such observables would be a more sensitive tool than the unpolarized differential cross section to figure out whether the kind of nonperturbative ingredients (diquarks, effective constituent masses) which are taken into account in our perturbative approach, are already sufficient or whether much more non-perturbative physics is still at work at a few GeV of momentum transfer. But also without using polarized beams or targets additional information on the validity and limitations of a perturbative mechanism could be attained just by measuring the angular decay distribution of the Φ and determining the corresponding spin-density matrix elements. Our predictions for ρ^0_{00}, $\Re(\rho^0_{10})$, and ρ^0_{1-1} at $p^{\gamma}_{\rm lab}=6$ GeV are shown in Fig. 8. This should be compared with the leading order perturbative result which is identically 1 for ρ^0_{00} and which vanishes in the case of ρ^0_{10} and ρ^0_{1-1} since the production of transversally polarized Φ's is already suppressed by at least $\mathcal{O}(m_H/\sqrt{\hat{s}})$. It should also be mentioned that the few data around $|t|\approx 1$ GeV^2 of Barber *et al.* [37] seem to reflect the small $|t|$ trend of our predicitions.

At the end of this section we want to comment on the perspective to extend this calculation to photoproduction of J/ψ. It is a simple matter, since we have already assumed a flavor dependent DA for the vector meson [cf. Eq. (2.10)]. The only thing to do is to replace the Φ mass by the J/ψ mass and the decay constant f^{Φ} by $f^{J/\psi}$. One, however, has to keep in mind that we have applied an expansion in the parameter $(m_H/\sqrt{\hat{s}})$. In order that this parameter is approximately of the same size in Φ and J/ψ production the photon laboratory energy has to be increased approximately by a factor $(m_{J/\Psi}/m_{\Phi})^2=9.2$ when going from Φ to J/ψ. A second criterion for the reliability of our approximate treatment of mass effects is that the coefficient of the first mass correction term should become small compared to the leading order. This coefficient is angular dependent and becomes large at small scattering angle. That means, if the size of the mass corrections relative to the leading order should be about the same in Φ and J/ψ production [$(m_H/\sqrt{\hat{s}})$ comparable], one has to consider much larger momentum transfers for J/ψ than for Φ production. A more detailed discussion of this point along with some numerical results can be found in Ref. [43]. A possible way to apply the perturbative approach to J/ψ production at a few GeV of momentum transfer would be to retain our prescription for the choice of the effective masses, but to refrain from the final expansion in $(m_H/\sqrt{\hat{s}})$. This has not been attempted yet since the analytical expressions for the amplitudes become very lengthy and the treatment of propagator singularities in the convolution integral, Eq. (2.1), becomes much more involved.

V. SUMMARY AND CONCLUSIONS

We have investigated the reaction $\gamma p \to \Phi p$ in the few-GeV momentum transfer region where unpolarized differential cross-section data from the CEBAF-93-031 experiment at JLAB are expected to become available very soon. Our theoretical approach is based on perturbative QCD supplemented by the assumption that baryons can be treated as quark-diquark systems. The same approach has already been successfully applied to other photon-induced hadronic reactions [15–19]. The motivation for introducing diquarks is, above all, to extend the perturbative approach from large down to moderately large momentum transfers. There are mainly two reasons why this can be achieved with diquarks. First, the overall momentum transfer has to be shared between less hadronic constituents than in the pure quark HSA. Hence the gluons which keep the hadronic constituents collinear are on the average harder and thus the running strong coupling constant becomes smaller. The second reason is that a certain class of non-perturbative effects, namely quark-quark correlations inside a baryon, is effectively accounted for by means of diquarks. The fact that a heavy quarkonium is produced in the final state entails a considerable reduction in computational effort. Only a small fraction of the Feynman diagrams which contribute in general to photoproduction of arbitrary mesons occurs in Φ production. To be more specific, these are just those diagrams in which the photon fluctuates into the heavy quark-antiquark pair which is then connected to the quark and the diquark in the proton via the exchange of two gluons, respectively. Both the scalar and vector-diquark components of the proton have been taken into account. We have also improved the diquark model in the sense that hadron-mass effects in the hard-scattering amplitude have been included in a systematic way. This has been accomplished by assigning to each hadronic constituent an effective mass xm_H (here x denotes the longitudinal momentum fraction of the constituent) and expanding the scattering amplitude in the small parameter $(m_H/\sqrt{\hat{s}})$. Only the leading and next-to-leading order terms in this expansion have been kept. The leading-order term provides for the hadron-helicity-conserving amplitudes and agrees, of course, with the massless result. The next-to-leading order term represents a power-correction and gives rise to non-vanishing hadron-helicity-flip amplitudes. It enables us to make predictions for polarization observables which require the flip of a hadronic helicity such as, e.g., the target asymmetry or the recoil polarization. We want to point out that our treatment of mass effects still preserves gauge invariance with respect to the photon and the gluon.

Our numerical studies have been performed with the diquark-model parameters and the quark-diquark DAs proposed in Ref. [15]. The DA of the Φ meson has been taken from the literature [23]. It satisfies QCD sum-rule constraints. Hence we have been able to make predictions without introducing new parameters. We have paid special attention to the correct and numerically robust treatment of propagator singularities. In the absence of large-t data ($t \gtrsim 4$ GeV^2) our results can only be compared with the available data which go up to $t \approx 1.5$ GeV^2. Our predictions for the differential cross section at two rather different photon energies ($p^{\gamma}_{\rm lab} = 6$ GeV and 2600 GeV) which are typical for CEBAF and HERA, respectively, occur still within the range of an extrapolation of the existing low-t data. It is worth mentioning that the predictions of a two-gluon-exchange model, in which the gluons are considered as a remnant of the Pomeron [35], become comparable to our result for $t \gtrsim 4$ GeV^2 if the gluons are allowed to couple to different quarks in the proton. This is not surprising because contributions in which all the hadronic constituents are (approximately) kept collinear by means of gluon exchange to prevent the hadrons from breaking up become increasingly important as soon as one enters the hard-scattering domain. Just those contributions are assumed to be the dominant ones within our HSA-based diquark model. We have also investigated within our model whether the (asymptotic) s^{-7} scaling behavior of the differential cross section at fixed angle is already realized for s values between 10 and 40 GeV. After dividing out the strong running coupling (which occurs to the sixth power in the cross section) an approximate s^{-7} scaling has been found. Our investigation of hadron-mass effects has revealed that they are still non-negligible in the few-GeV momentum transfer range and photon energies of the order of 10 GeV. Correspondingly, also polarization observables which require the flip of a hadronic helicity, like the target polarization, occur to be sizable. Finally, we have considered the possibility to extend the present calculation to photoproduction of J/ψ mesons. In order that our treatment of mass effects remains reliable for J/ψ's one has to go to much larger energies and momentum transfers where experimental data cannot be expected. The situation with respect to the momentum transfer could perhaps be improved by refraining from the final expansion in $(m_H/\sqrt{\hat{s}})$. This, however, will considerably complicate the treatment of propagator singularities and make the analytical expressions for the amplitudes much more complicated. Therefore it has not been attempted as yet.

Our diquark-model calculations for $\gamma p \to \Phi p$ will meet the first severe test in the near future when the data analysis of the CEBAF 93-031 experiment will be completed. With these data, which go up to t values of about 5 GeV^2, one will get a first glimpse of how different production mechanisms (Pomeron exchange → gluon exchange → hard-scattering mechanism) in high-energy photoproduction evolve with increasing momentum transfer. However, in order to really touch the hard-scattering domain much higher photon energies than those which can be reached at the present stage of CEBAF would be desirable. In addition to unpolarized differential cross sections, polarization observables, which require the flip of hadronic helicities, could serve as an indicator for the relative importance of hard and soft photoproduction mechanisms, since hard scattering is closely connected with hadronic helicity conservation.

ACKNOWLEDGMENTS

C.F.B. would like to thank the Paul-Urban-Stipendienstiftung for supporting a visit at the Institute of Theoretical Physics at the University of Graz during which part of this paper has been completed.

[1] G. Audit *et al.*, CEBAF Proposal No. 93-031, 1993.
[2] J. A. Crittenden, *Exclusive Production of Neutral Vector Mesons at the Electron-Proton Collider HERA*, Springer Tracts in Modern Physics Vol. 140 (Springer, Berlin, 1997).
[3] A. Donnachie and P. V. Landshoff, Phys. Lett. B **348**, 213 (1995).
[4] A. Donnachie and P. V. Landshoff, Phys. Lett. B **185**, 403 (1987).
[5] A. Donnachie and P. V. Landshoff, Nucl. Phys. **B311**, 509 (1989).
[6] J. C. Collins, L. Frankfurt, and M. Strikman, Phys. Rev. D **56**, 2982 (1997).
[7] M. Diehl, T. Feldmann, R. Jakob, and P. Kroll, Eur. Phys. J. C **8**, 409 (1999).
[8] For a comprehensive review of hard exclusive processes and further references see, e.g., S. J. Brodsky and G. P. Lepage, in *Perturbative Quantum Chromodynamics*, edited by A. H. Mueller (World Scientific, Singapore, 1989).
[9] V. L. Chernyak and A. R. Zhitnitsky, Phys. Rep. **112**, 173 (1984).
[10] N. Isgur and C. H. Llewellyn Smith, Nucl. Phys. **B137**, 526 (1989).
[11] J. Bolz *et al.*, Z. Phys. C **66**, 267 (1995).
[12] J. Gronberg *et al.*, Phys. Rev. D **57**, 33 (1998).
[13] J. Bolz and P. Kroll, Z. Phys. A **356**, 327 (1996).
[14] A. V. Radyushkin, Phys. Rev. D **58**, 114008 (1998).
[15] R. Jakob, P. Kroll, M. Schürmann, and W. Schweiger, Z. Phys. A **347**, 109 (1993).
[16] P. Kroll, Th. Pilsner, M. Schürmann, and W. Schweiger, Phys. Lett. B **316**, 546 (1993).
[17] P. Kroll, M. Schürmann, and P. A. M. Guichon, Nucl. Phys. **A598**, 435 (1996).
[18] C. F. Berger, diploma thesis, Technological University Graz, 1997.
[19] P. Kroll, M. Schürmann, K. Passek, and W. Schweiger, Phys. Rev. D **55**, 4315 (1997).
[20] R. Jakob, Phys. Rev. D **50**, 5647 (1994).
[21] T. Huang, Nucl. Phys. B (Proc. Suppl.) **7**, 320 (1989).
[22] J. J. Aubert *et al.*, Phys. Lett. **97B**, 306 (1980).
[23] M. Benayoun and V. L. Chernyak, Nucl. Phys. **B329**, 285 (1990).
[24] M. Wirbel, B. Stech, and M. Bauer, Z. Phys. C **29**, 637 (1985).
[25] T. Feldmann and P. Kroll, Phys. Lett. B **413**, 410 (1997).
[26] M. Neubert and B. Stech, in *Heavy Flavours II*, edited by A. J. Buras and M. Lindner (World Scientific, Singapore, 1998), hep-ph/9705292.
[27] G. R. Farrar, G. Sterman, and H. Zhang, Phys. Rev. Lett. **62**, 2229 (1989).
[28] C. Carimalo, N. Arteaga-Romero, and S. Ong, Eur. Phys. J. C **11**, 685 (1999).
[29] M. Anselmino, F. Caruso, and F. Murgia, Phys. Rev. D **42**, 3218 (1990).
[30] M. Pichowsky, Ç. Şavkli, and F. Tabakin, Phys. Rev. C **53**, 593 (1996).
[31] C. Bourrely, E. Leader, and J. Soffer, Phys. Rep. **59**, 95 (1980).
[32] J. Küblbeck, M. Böhm, and A. Denner, Comput. Phys. Commun. **60**, 165 (1990).
[33] R. Mertig, M. Böhm, and A. Denner, Comput. Phys. Commun. **64**, 345 (1991).
[34] J.-M. Laget and R. Mendez-Galain, Nucl. Phys. **A581**, 397 (1995).
[35] J.-M. Laget, Report No. DAPNIA/SPhN-98-54, 1998.
[36] J. Ballam *et al.*, Phys. Rev. D **5**, 3150 (1973).
[37] D. P. Barber *et al.*, Z. Phys. C **12**, 1 (1982).
[38] R. L. Anderson *et al.*, Phys. Rev. D **14**, 679 (1976).
[39] M. Derrik *et al.*, Phys. Lett. B **377**, 259 (1996).
[40] C. Carimalo and S. Ong, Z. Phys. C **52**, 487 (1991).
[41] Q. Zhao, J.-P. Didelez, M. Guidal, and B. Saghai, Nucl. Phys. **A660**, 323 (1999).
[42] A. I. Titov, Y. Oh, S. N. Yang, and T. Morii, Phys. Rev. C **58**, 2429 (1998).
[43] C. F. Berger and W. Schweiger, in Proceedings of the INT/JLab Workshop on Exclusive and Semi-Exclusive Processes at High Momentum Transfer, Newport News, 1999, hep-ph/9909270.